Zero Temperature Spin Wave Damping in Spin Polarized ^{3}He: Does It Exist?

Gerard Vermeulen and Agnès Roni

Centre de Recherches sur les Très Basses Températures, Laboratoire Associé à l'Université Joseph Fourier, BP 166, Grenoble Cédex 9, France

(Received 5 September 2000)

Previous spin echo experiments at equilibrium polarizations in ^{3}He-^{4}He mixtures have confirmed the prediction of zero temperature polarization-induced spin wave damping in Fermi liquids. We have measured the damping of spin waves in dilute ^{3}He, spin polarized by a ^{4}He circulating dilution refrigerator. The maximum polarization is almost a factor of 5 higher than the equilibrium polarization in a magnetic field of 10.54 T at temperatures between 10 and 25 mK. The spin wave damping is much smaller than expected on the basis of the spin echo experiments and shows that the existence of polarization-induced spin wave damping is an open question.

DOI: 10.1103/PhysRevLett.86.248 PACS numbers: 67.65.+z, 67.57.Lm, 67.60.–g

The spin dynamics in weakly polarized Fermi liquids gives rise to many unusual features and is very well described by the Leggett equations [1]. These features, including anomalous spin echo behavior (the Leggett-Rice effect) [2] and spin waves [3], are observable in the collisionless regime where the Landau molecular field exceeds the inverse of the quasiparticle relaxation time. The Landau field is proportional to the polarization and, since the scattering phase space is restricted to a shell of width k_BT around the Fermi surface, the quasiparticle relaxation time is proportional to $1/T^2$. We address the problem of spin dynamics in Fermi liquids at polarizations higher than those achieved in previous investigations.

A polarized Fermi liquid is characterized by two different Fermi surfaces for the quasiparticles with a spin parallel or antiparallel to the polarization, but the Leggett equations have been derived assuming a weak polarization and therefore only one Fermi surface. Meyerovich has raised the fundamental point that extension of the Leggett equations to higher polarization requires the introduction of a longitudinal and a transverse quasiparticle relaxation time, $\tau_\parallel$ and $\tau_\perp$ [4]. The evolution of a gradient in the magnitude of the spin density is controlled by the longitudinal relaxation time, still proportional to $1/T^2$. The decay rate of the transverse component of the spin density, precessing around the external magnetic field, is governed by the transverse relaxation time. The transverse relaxation time remains finite at $T = 0$ K, because dephasing of the transverse component of the spin density in a field gradient creates quasiparticles in a mixed state up-down, opening up the whole phase space between the two Fermi surfaces for scattering. This idea has been pursued in theoretical studies in dense [5] and dilute Fermi liquids [6]. In the low polarization limit, the transverse relaxation time may be parametrized by $1/\tau_\perp \propto T^2 + T_a^2$, where the anisotropy temperature T_a is *proportional to the polarization* [6,7]. The theory for very dilute mixtures [6] leads in this limit to the expression $T_a = \hbar\gamma B/2\pi k_B$ at equilibrium polarization. In our experimental conditions $T_a(10.54\ \text{T}) = 2.7$ mK, where we will always give the value of the external field between parentheses.

According to Fomin, this approach does not take into account that the magnitude of the local spin density is a conserved quantity and that the local spin density and the Landau field precess together. If the variations of the Landau field are slow and have a small amplitude, they can be treated as an adiabatic perturbation and do not give rise to scattering. He has derived a spin wave dispersion relation at $T = 0$ K, which contains no damping up to second order in the wave vector [8].

Several spin echo experiments, all at saturated vapor pressure, confirm that the quasiparticle relaxation time behaves as $1/\tau_\perp \propto T^2 + T_a^2$. An anisotropy temperature of $T_a(8\ \text{T}) = 16.4 \pm 2.2$ mK has been measured in pure liquid ^{3}He [9]. Ager *et al.* have observed a difference between $\tau_\parallel$ and $\tau_\perp$ in several ^{3}He-^{4}He mixtures with $T_a(8.8\ \text{T}) = 19 \pm 3$ mK at a ^{3}He concentration of 6.4% [10]. Although the experimental anisotropy temperatures are rather high with respect to theory, these experiments have been considered a proof in favor of the existence of zero temperature spin wave damping. The difference between the experimental results and the prediction of Jeon and Mullin for the very dilute mixtures is attributed to the Fermi liquid interactions [7,9,10]. Later experiments have resulted in lower values for the anisotropy temperature at higher fields: $T_a(11.3\ \text{T}) = 12 \pm 2$ mK and 13 ± 2 mK for pure ^{3}He [11] and a 6.2% ^{3}He-^{4}He mixture [12]. This raises the question, why is the ensemble of experimental results inconsistent with the prediction that T_a is proportional to the polarization?

To approach this problem from a different angle, we have measured the spin wave damping in a device giving an enhancement of the polarization by a factor $A \leq 5$ with respect to its equilibrium value (2.6% for the dilute phase at 7 bars). Consequently, within the context of the theories predicting zero temperature spin wave damping, any polarization induced spin wave damping should also be amplified. To make the predicted dependence on the polarization

 0031-9007/01/86(2)/248(4)$15.00

enhancement factor, A, explicit, we write $T_a = AT_{a0}$ and $1/\tau_\perp \propto T^2 + A^2T_{a0}^2$, where T_{a0} denotes the anisotropy temperature for the equilibrium polarization in a magnetic field, B_0.

We also amend the spin wave equation [1] for the polarization enhancement factor, A:

$$i\,\frac{\partial\sigma^+(\mathbf{r},t)}{\partial t} = \left[\frac{iD_\perp}{1 + i\lambda A\omega\tau_\perp}\nabla^2 + \gamma B(\mathbf{r})\right]\sigma^+(\mathbf{r},t)\,, \tag{1}$$

where σ^+ is the transverse spin density, $D_\perp = v_F^2(1 + F_0^a)\tau_\perp/3$ is the transverse spin diffusion coefficient, $\lambda = (1 + F_0^a)^{-1} - (1 + F_1^a/3)^{-1}$ accounts for the Fermi liquid interactions, and $\omega(\mathbf{r}) = \gamma B(\mathbf{r})$ corresponds to the applied magnetic field. This interpretation of Leggett's equation is implicit in his derivation of the Leggett-Rice effect [1].

The experiments have been performed on the dilute phase in the mixing chamber of a ^{4}He circulating dilution refrigerator. Diluting ^{3}He into ^{4}He in a magnetic field at a pressure above 2.6 bars *cools and polarizes* both phases in the mixing chamber [13]. Figure 1 shows that the mixing chamber consists of two cells. When ^{4}He is injected, the upper cell fills with a saturated ^{3}He-^{4}He mixture. The lower cell remains almost entirely filled with concentrated—nearly pure—^{3}He, except for dilute phase droplets falling from the capillary between the two cells. The dilution process takes place in the lower cell at the phase boundary of each new droplet before it falls. Both cells are coupled by the diffusion of heat and polarization through the capillary. The polarizer does not allow the polarization and temperature to vary independently. Without ^{4}He injection, the polarization of the liquid inside both cells relaxes to its equilibrium value at a temperature of about 30 mK. After starting the ^{4}He injection, the polarization increases with a time constant on the order of 1 h towards its stationary out of equilibrium value. Initially, both phases in each cell cool and polarize rapidly. Then, the temperature, measured by vibrating wire viscometers [13,14] in both cells, rises slowly with the heat production due to the out of equilibrium polarization. The temperature increase in the upper cell is more important than in the lower one; the temperature difference between the two cells increases from 2 to almost 10 mK.

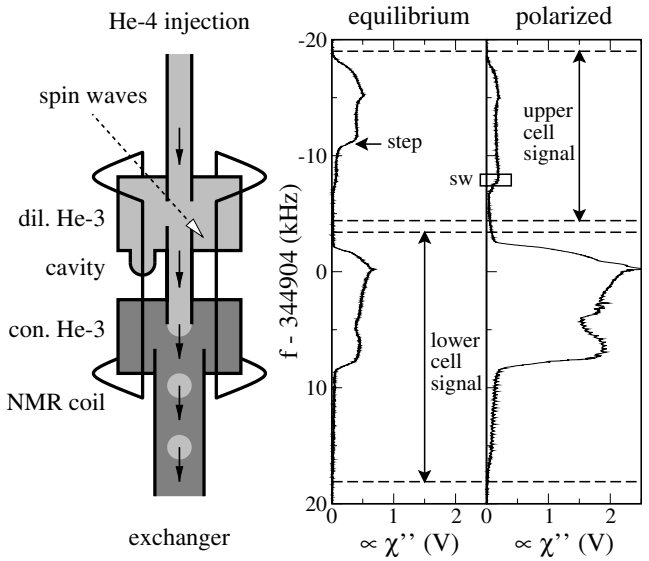

FIG. 1. Left: the mixing chamber consisting of a dilute and a concentrated ^{3}He cell. Right: continuous wave NMR spectra in a field of 10.54 T and a field gradient of -10.6 ± 0.5 G/cm. The left spectrum has been taken without ^{4}He injection, when the polarization is in equilibrium with the external field. Some concentrated phase has entered the upper cell and floats on the dilute phase: the step in the absorption signal at -11 kHz is due to the magnetization difference between both phases. The right spectrum, taken a few hours after starting to inject ^{4}He, shows that the upper cell is now full of dilute phase. The polarization has grown by a factor $A = 3.93$ in both cells. We focus on the spin waves in the region indicated by the dashed arrow. They are barely visible within the box labeled SW in the right spectrum.

An NMR coil tuned to a frequency of 344.9 MHz surrounds both cells. The spectrometer allows us either to obtain the full NMR spectrum by sweeping the frequency or to zoom in on the spin wave modes by low power pulsed NMR. The tipping angle is estimated to be less than 1 deg for a pulse length of 0.4 ms. The polarization enhancement is obtained by normalizing the integral of the absorption signal from the lower cell to its value at equilibrium. The absorption signals of the concentrated and dilute phase vary proportionally, showing that the polarization enhancement in both cells is the same.

The literature describes algorithms to calculate the resonance frequencies and the half-widths of spin wave modes localized by a field gradient in rectangular [3] and spherical [15] cells. We will use the one-dimensional solution of Eq. (1) with one reflecting boundary at $z = 0$ and a magnetic field of the form $B(z) = \omega_0/\gamma + Gz$. The spin wave modes are given by Airy functions, $\mathrm{Ai}(-Z_N - z[\gamma G(1 + i\lambda A\omega_0\tau_\perp)/iD_\perp]^{1/3})$, where the $Z_{N=1,2,\ldots}$ are the zeros of the derivative of $\mathrm{Ai}(z)$. The complex eigenfrequencies, ω_N, are

$$\omega_N - \omega_0 = Z_N\left(\frac{\gamma^2G^2iD_\perp}{1 + i\lambda A\omega_0\tau_\perp}\right)^{1/3}, \tag{2}$$

or in the limit $\lambda A\omega_0\tau_\perp \gg 1$:

$$\omega_N - \omega_0 \approx Z_N\left(\frac{\gamma^2G^2D_\perp}{\lambda A\omega_0\tau_\perp}\right)^{1/3}\left(1 - \frac{1}{3i\lambda A\omega_0\tau_\perp}\right). \tag{3}$$

We write $\omega_N - \omega_0 \equiv \Delta\omega_N - i\delta\omega_N/2$, where $\Delta\omega_N$ is the "mode frequency" and $\delta\omega_N/2$ the half-width. In the limit $\lambda A\omega_0\tau_\perp \gg 1$, the mode frequency is given by $\Delta\omega_N \approx Z_N(\gamma^2G^2D_\perp/\lambda A\omega_0\tau_\perp)^{1/3}$ and does not depend on $\tau_\perp$ because $D_\perp \propto \tau_\perp$. The relation $-3(\delta\omega_N/2)/\Delta\omega_N \approx 1/\lambda A\omega_0\tau_\perp$ allows a determination of $\lambda\tau_\perp$.

Higher order magnetic field gradient terms and misalignment of the gradient with respect to a symmetry axis of

the experimental cell introduce submodes in the spin wave spectra [3]. The use of a spherical cavity has been successfully introduced to be insensitive to misalignments [15]. We have made a hemispherical cavity with a radius of 0.5 mm in the bottom of the upper cell. However, after careful shimming of the gradients in the x and y direction, the spin wave modes trapped against the bottom of the cylindrical cell are much easier to analyze than the modes that we observe in the cavity. The main features of the spin wave spectrum in the cylindrical cell are very well described by Eq. (2) and the submodes are easy to identify. Therefore, we focus on the modes in the cylindrical cell.

Figure 2 shows the first six main spin wave modes trapped against the bottom of the cylindrical cell at a pressure of 7 bars (at least 20 main modes are visible). The gradient is $G = -10.6 \pm 0.5$ G/cm, the average of $G = -11.2$ G/cm (from the specification of the gradient coil and the measured gradient of the main field) and $G = -10.1$ G/cm (from the linewidth and the size of the mixing chamber).

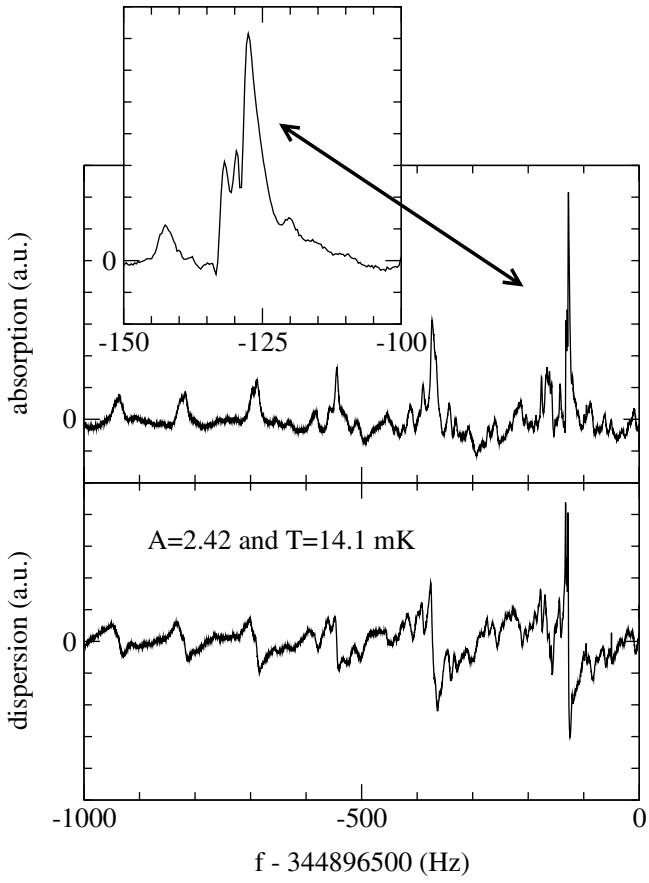

FIG. 2. Absorption and dispersion signal of the first 6 spin wave modes trapped by a field gradient of -10.6 G/cm against the bottom of the cell filled with dilute ^{3}He. The first mode (consisting of at least 3 submodes) is shown in the inset at a $10\times$ larger frequency scale. To estimate the half-width of the modes, we have taken into account that each mode consists of several submodes due to imperfections in geometry and gradient: the width of each largest amplitude submode has been determined from the frequency difference between the minimum and maximum of its dispersion signal. In this way, we obtain $\delta f_N/2 = 1.6$ Hz for the first mode.

Data for the spin diffusion coefficient, $D_\perp$, and the Landau molecular field parameters, $\lambda\tau_\perp$, in dilute saturated ^{3}He are not available at pressures where polarizing by dilution works. We compare our results with an extrapolation of low field spin diffusion data at 7 bars [16] to the saturation concentration, $x_s = 9.3\%$. We extrapolate $D_\perp T^2 = 69.5 \times 10^{-6}$ cm^2 K^2/s and $\lambda\tau_\perp T^2 = 1.8 \times 10^{-12}$ s K^2 with an estimated error of 10%.

Figure 3 compares the mode frequencies, $\Delta f_N \equiv \Re(f_N - f_0)$, and half-widths, $\delta f_N/2 \equiv -\Im(f_N - f_0)$, from two typical spectra at different ambient temperatures with Eq. (2) for $T_{a0}(10.54\ \mathrm{T}) = 0$ and 5 mK. The experimental value of the NMR frequency at the cell bottom, f_0, cannot be determined precisely from our NMR data. Therefore, it is chosen such that Δf_1 is given by its calculated value. Then, the experimental and calculated values of Δf_N coincide within 2%, showing good agreement with the extrapolated ratio $D_\perp/\lambda\tau_\perp$ and assuring that we know $\lambda\tau_\perp$ indeed to within 10%.

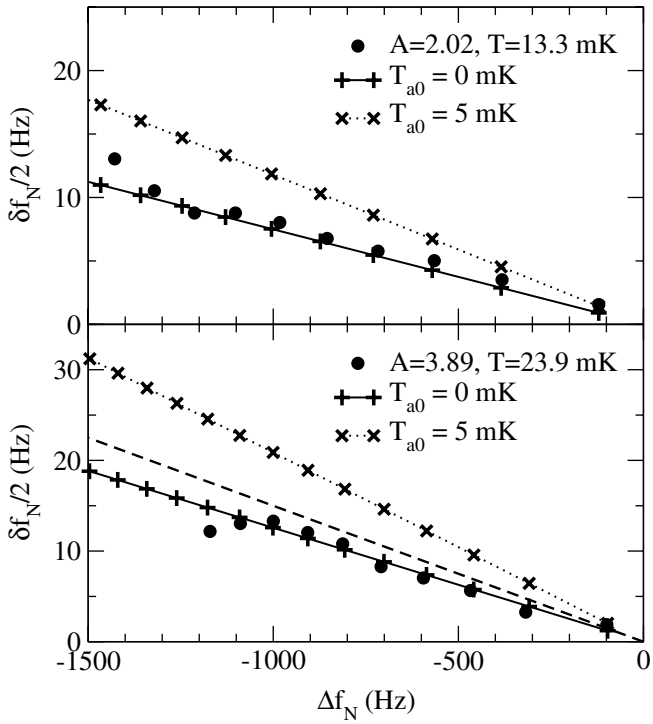

FIG. 3. Comparison between experimental (●) and calculated values of the mode frequencies, Δf_N, and half-widths, $\delta f_N/2$, of the spin wave modes for spectra with $A = 2.02$, $T = 13.3$ mK (upper graph) and with $A = 3.89$, $T = 23.9$ mK (lower graph). Input for the calculation is $G = -10.6$ G/cm, $D_\perp T^2 = 69.5 \times 10^{-6}$ cm^2 K^2/s, $\lambda\tau_\perp T^2 = 1.8 \times 10^{-12}$ s K^2, $T_{a0}(10.54\ \mathrm{T}) = 0$ mK (+), and $T_{a0}(10.54\ \mathrm{T}) = 5$ mK (×). The calculated modes are characterized by the relation $-3(\delta f_N/2)/\Delta f_N = (T^2 + A^2 T_{a0}^2)/1.8 \times 10^{-12} A\omega_0$. The experimental data in the upper graph is consistent with $\lambda A\omega_0\tau_\perp \simeq 44.5$.

Our main result is the good agreement between the experimental half-widths and the calculation with $T_{a0}(10.54\ \mathrm{T}) = 0$ mK. Before discussing the implications, we recall that the slope $(\delta f_N/2)/\Delta f_N$ equals $-1/3\lambda A\omega_0\tau_\perp$. So, the polarization and temperature dependence of the calculated modes is described by $-3(\delta f_N/2)/\Delta f_N = (T^2 + A^2T_{a0}^2)/1.8 \times 10^{-12}A\omega_0$.

To compare the latest Nottingham result—$T_{a0}(11.3\ \mathrm{T}) = 13 \pm 2$ mK for a 6.2% mixture at $p = 0$ bars [12]—with ours, we scale it for the difference in magnetic field and polarizability [13] and find $T_{a0}(10.54\ \mathrm{T}) \simeq 10$ mK instead of 0 mK. The vertical axes in Fig. 3 have to be expanded by a factor of 5–6 to show all modes calculated with $T_{a0}(10.54\ \mathrm{T}) \simeq 10$ mK. We dismiss three explanations for this discrepancy: (1) Fermi liquid interactions may enhance T_{a0} [7,9] and possibly in a pressure dependent way. In view of the weak pressure dependence of the known Fermi liquid parameters in dilute ^{3}He, we consider it unlikely that such a large discrepancy may be explained by the pressure difference. (2) The results of the spin echo experiments may differ, because they have been obtained at equilibrium polarizations [12]. We point out that after the π pulse (50% of the duration of a spin echo experiment) the polarization is inverted and far from equilibrium. (3) The dipolar field gives rise to magnetostatic modes in pure ^{3}He [11,17] and may affect the spin wave spectrum in dilute ^{3}He. Inclusion of the dipolar field in the calculation of spin wave spectra in a sphere results in changes that are barely visible for our sample [18]. We expect that the effect of the dipolar field is also negligible in our geometry.

The data for $\delta f_N/2$ look smaller than calculated using $T_{a0}(10.54\ \mathrm{T}) = 2.7$ mK, the prediction of the dilute Fermi gas model [6], and indicated by the dashed line in the lower graph in Fig. 3. However, a possible decrease of 10% in temperature or an unlikely increase of 20% in $\lambda\tau_\perp$ would resolve the discrepancy with this model.

In conclusion, our results on spin wave damping in dilute ^{3}He disagree significantly with previous results from spin echo experiments. Ours agree with Fomin's prediction that polarization induced spin wave damping does not exist. In the present experiment, our errors are still too large to totally rule out the dilute Fermi gas model, however. To further test the existence of zero temperature polarization induced spin wave damping, experiments at higher polarizations and lower temperatures are needed.

We thank O. Buu, I. A. Fomin, P. L. Krotkov, V. P. Mineev, and P. E. Wolf for many discussions, and M. Chapellier, J. Flouquet, and J. Joffrin for the loan of experimental equipment.

[1] A. J. Leggett, J. Phys. C **3**, 448 (1970).
[2] L. R. Corrucini, D. D. Osheroff, D. M. Lee, and R. C. Richardson, J. Low Temp. Phys. **8**, 229 (1972).
[3] D. Candela, N. Masuhara, D. S. Sherill, and D. O. Edwards, J. Low Temp. Phys. **63**, 369 (1986).
[4] A. E. Meyerovich, Phys. Lett. **107A**, 177 (1985).
[5] A. E. Meyerovich and K. A. Musaelian, J. Low Temp. Phys. **89**, 781 (1992); **94**, 249 (1994); **95**, 789 (1995).
[6] W. J. Mullin and J. W. Jeon, J. Low Temp. Phys. **88**, 433 (1992); J. W. Jeon, Ph.D. thesis, University of Massachusetts, 1989.
[7] A. E. Meyerovich and K. A. Musaelian, Phys. Rev. Lett. **72**, 1710 (1994).
[8] I. A. Fomin, JETP Lett. **65**, 749 (1997).
[9] L-J. Wei, N. Kalechofsky, and D. Candela, Phys. Rev. Lett. **71**, 879 (1993).
[10] J. H. Ager, A. Child, R. König, J. R. Owers-Bradley, and R. M. Bowley, J. Low Temp. Phys. **99**, 683 (1995).
[11] D. Candela, H. Akimoto, R. M. Bowley, O. Buu, D. Clubb, and J. R. Owers-Bradley, J. Low Temp. Phys. (to be published).
[12] J. R. Owers-Bradley, R. M. Bowley, O. Buu, D. Clubb, and G. Vermeulen, J. Low Temp. Phys. (to be published).
[13] A. Rodrigues and G. Vermeulen, J. Low Temp. Phys. **108**, 103 (1997).
[14] The temperature and pressure dependent viscosity in the dilute phase with a saturation concentration x_{3s} is approximated by a phenomenological formula $\eta(T, p) = [x_{3s}(0, p)/x_{3s}(0, 0)]^{2/3}\eta(T, 0)$, where $\eta(T, 0)$ is given by J. C. H. Zeegers, A. T. A. M. de Waele, and H. M. Gijsman, J. Low Temp. Phys. **84**, 37 (1991). At $p = 10$ bars, this formula agrees within error bars with the value cited by R. König and F. Pobell, J. Low Temp. Phys. **97**, 287 (1994).
[15] D. Candela, D. R. McAllaster, and L-J. Wei, Phys. Rev. B **44**, 7510 (1991).
[16] H. Ishimoto, H. Fukuyama, T. Fukuda, T. Tazaki, and S. Ogawa, Phys. Rev. B **38**, 6422 (1988).
[17] A. Roni, Ph.D. thesis, Université Joseph Fourier, Grenoble, France, 1999.
[18] P. L. Krotkov, V. P. Mineev, and G. Vermeulen (to be published).